2024 IEEE 63rd Conference on Decision and Control (CDC)
December 16-19, 2024. MiCo, Milan, Italy

Maneuvering Control of Uncertain Nonlinear Systems: An Output Regulation Viewpoint

Yibo Zhang, Wentao Wu, Tao Xie, Peng Cheng, Di Wu and Weidong Zhang

Abstract— **Maneuvering control aims to drive the controlled system to achieve a desired motion along a parameterized path, where the path variable, a scalar, tunes additional dynamic tasks. In this paper, we investigate the maneuvering control problem of uncertain nonlinear systems from the perspective of output regulation. Initially, we demonstrate that the maneuvering control problem can be transformed into an output regulation problem. Then, we design a controller for maneuvering control based on the internal model principle and a neural predictor-based dynamic surface control method. We prove that the resulting closed-loop system is input-to-state stable. The effectiveness of proposed theoretical results is verified via a simulation example.**

I. Introduction

Controlling an object is an academic issue that is both historical and novel [1]–[12]. In particular, tracking is an important topic, which involves steering a controlled system along a given trajectory, also known as trajectory tracking. Trajectory tracking can achieve a desired spatial motion of the controlled system at the geometric level, but it may be incapable of handling some special constraints.

In many practical applications, based on the implementation of trajectory tracking, the controlled system may also need to meet other conditions during the tracking process [1]. For example, an unmanned surface vehicle can be driven to move along a predefined trajectory, but it needs to use different velocities and accelerations in several legs. To address similar issues, the concept of maneuvering control was introduced [1], [2]. Maneuvering control includes two tasks. The first one, called the geometric task, is to drive the controlled system along a given parameterized path, which is similar to the main idea of trajectory tracking. The second one, called the dynamic task, is to drive a manually defined path variable to achieve some desired performance specifications via constructing an appropriate timing law. In some existing results, maneuvering control is also known as path maneuvering or path following.

Early research primarily focused on the mathematical principles underpinning maneuvering control, as seen in [1]–[3]. Subsequently, in recent years, maneuvering control has been applied in different fields, such as multi-agent systems [4]–[6], unmanned surface vehicles [7]–[9], VTOL vehicles [11], robots [10], and unmanned aerial vehicles [12]. Despite the variety of communication strategies, formation tasks, and controlled systems considered in these studies [1]–[12], they share two common features. First, for the geometric task, these methods [1]–[12] can implement the desired motion using control strategies suitable for trajectory tracking, such as backstepping or LMI-based control. Second, for the dynamic task, these existing methods [1]–[12] have designed various forms of variable update laws to ensure the path and path variable are smoothly updated.

Like maneuvering control, output regulation is a crucial method that facilitates the output to converge more effectively to the desired signal [13]–[15]. Output regulation also enables the achievement of the dynamic task. When the path updates smoothly, it can be regarded as a desired exogenous signal generated by an exosystem. In [6], an output-feedback consensus maneuvering controller is designed for strict-feedback nonlinear systems, in which the parameterized path is transformed into a linear dynamics representation. However the controller in [6] has an LMI-based structure.

In light of the preceding observations, in this paper, we consider the maneuvering control problem of a class of uncertain nonlinear systems from an output regulation perspective. Distinct from the existing results on maneuvering control, the main contributions of this paper are twofold.

- We demonstrate that the maneuvering control problem, as discussed in [1]–[9], can be recast as a specific output regulation problem. Adopting this perspective allows for the application of the internal model principle in the design of maneuvering control strategies. Furthermore, we propose a general framework for designing such controllers for uncertain nonlinear systems within the viewpoint of output regulation.
- Within the proposed control framework, we demonstrate the design of a nonlinear maneuvering controller using a neural predictor-based dynamic surface control (DSC) method and the internal model principle. The complexity of this controller has not significantly increased.

II. Notation

$\underline{\lambda}(\cdot)$ and $\bar{\lambda}(\cdot)$: minimal and maximal eigenvalues of a matrix respectively; $A \succ 0$: A is a positive definite matrix; diag$\{\cdot\}$: a diagonal matrix; I_m: m by m unitary matrix; O_m: m by m zero matrix; $\mathbb{R}^n$: n-dimensional Euclidean Space; $\mathbb{R}^+$: positive real scalar; $f^{(l)}(\cdot)$: the lth-order derivative of $f(\cdot)$; $\|\cdot\|$ and $\|\cdot\|_{\mathrm{F}}$: Euclidean norm and the Frobenius norm

This paper is supported by National Key R&D Program of China (2022ZD0119903), National Natural Science Foundation of China (U2141234, 52201369), Shanghai Science and Technology Program (22015810300), and Oceanic Interdisciplinary Program of Shanghai Jiao Tong University (SL2022PT112). (Corresponding Author: Weidong Zhang).

The authors are with Department of Automation, Shanghai Jiao Tong University, Shanghai, 200240, China. Yibo Zhang is also with Department of Automation, Shanghai University, Shanghai, 200444, China. Di Wu is also with PRISMA Lab, Department of Engineering and Information Technology, University of Naples Federico II, 80125 Naples, Italy. zhang297,wdzhang@sjtu.edu.cn

respectively; $L^l f(\cdot)$: the lth-order Lie derivative of $f(\cdot)$; $\otimes$: Kronecker product.

III. Problem Formulation

In this section, a brief formulation about maneuvering control is given. Consider an uncertain nonlinear system

$$\begin{cases} \dot{x}_k = x_{k+1} + f_k(\bar{x}_k), \quad k = 1, ..., n-1 \\ \dot{x}_n = u + f_n(\bar{x}_n) \\ y = x_1 \end{cases} \tag{1}$$

where $x_k \in \mathbb{R}^m$ and $x_n \in \mathbb{R}^m$ are state variables, k denotes the index, $u \in \mathbb{R}^m$ is the control input variable, $y \in \mathbb{R}^m$ is the output variable, $f_k(\bar{x}_k) : \mathbb{R}^{km} \to \mathbb{R}^m$ and $f_n(\bar{x}_n) : \mathbb{R}^{mn} \to \mathbb{R}^m$ are unknown nonlinear smooth vector functions with $\bar{x}_k = [x_1, ..., x_k]^{\mathrm{T}} \in \mathbb{R}^{km}$, $\bar{x}_n = [x_1, ..., x_n]^{\mathrm{T}} \in \mathbb{R}^{mn}$.

In the maneuvering control problem, the controlled system is designed to steer along a desired parameterized path $y_r(\theta)$. In a leader-following setup, $y_r(\theta)$ can be seen as the virtual leader. The scalar θ denotes a path variable.

The control objectives of maneuvering control include both a geometric task and a dynamic task. The mathematics are expressed as follows:

- **Geometric task** is to drive the controlled system to track the desired parameterized path as far as possible

$$\lim_{t \to +\infty} \|y - y_r(\theta)\| \leq \varepsilon_g \tag{2}$$

  where $\varepsilon_g \in \mathbb{R}^+$ denotes a residual error.
- **Dynamic task** is to force the path variable θ to satisfy the additional objectives:
  1. Time objective:

$$\lim_{t \to +\infty} |\theta(t) - v_t(t)| \leq \varepsilon_t \tag{3}$$

  where $v_t(t) \in \mathbb{R}^+$ denotes a desired time signal and $\varepsilon_t \in \mathbb{R}^+$ denotes a residual error. Eq. (3) means that θ will converge to v_t as far as possible.
  2. Arbitrary order objective: For $t \geq 0$, we have

$$|\theta^{(k)}(t) - v_a(\theta(t), \dot{\theta}(t), ..., \theta^{(k-1)}(t), t)| \leq \varepsilon_a \tag{4}$$

  where $v_a(\cdot) \in \mathbb{R}^+$ denotes a desired tuning performance and $\varepsilon_a \in \mathbb{R}^+$ denotes a residual error. $v_a(\cdot)$ should be determined by the actual dynamic performance requirements. Eq. (4) means that $\theta^{(k-1)}$ will be forced to achieve the given performance of path update. For instance, when $k = 1$, the dynamic objective is to tune the velocity of the path update, and when $k = 2$, the dynamic is to tune the accelerate of the path update.

IV. Maneuvering control under the output regulation viewpoint

A. Path variable and path update law

Different from tracking control guided by the time-dependent trajectory $y_r(t)$, in maneuvering control, the path $y_r(\theta)$ is parameterized by the path variable θ. θ can be regarded as an additional control degree of freedom, and thus a path update law, defined as ω, needs to be designed to achieve the smooth update of θ. The dynamics of θ can be expressed as

$$\theta^{(k)} = g_\theta(\omega) \tag{5}$$

where $g_\theta(\omega) : \mathbb{R} \to \mathbb{R}$ is a smooth and continuous function.

Since θ is artificially defined, we can select a suitable $g_\theta(\omega)$ to ensure that the dynamics of θ are linear, because it is convenient for linear θ to stabilize and redesign. According to existing results, the model of θ can be represented by the following common types of linear models

1). First-order dynamics [1]

$$\dot{\theta} = \omega. \tag{6}$$

2). First-order tracking dynamics [2], [4], [5], [7], [8]

$$\dot{\theta} = v_a(\theta_t, t) - \omega. \tag{7}$$

The first-order and first-order tracking dynamics can be utilized to achieve time and velocity objectives.

3). lth-order dynamics [3], [6]

$$\theta^{(l)} = \omega, \quad l = 1, 2, ..., m. \tag{8}$$

The lth-order dynamics can be utilized to achieve the arbitrary order objective. In general, the order of θ-system is less than the order of the controlled system.

Because the dynamics of θ is linear, the path update law ω can be designed with ease. To achieve the dynamic objective, ω is associated with the path variable θ, the desired objectives v_a or (v_t, v_s), and path information $y_r(\theta), \dot{y}_r(\theta), \ldots, y_r^{(l-1)}(\theta)$. In some existing results, $y_r(\theta)$ is stored in the controlled system. The path update may also be influenced by the controlled system in such applications, allowing the output y of the controlled system to be utilized in ω. The form of ω can be expressed as follows

$$\omega = g_\omega(\theta, v_a(\cdot), y, y_r(\theta), \dot{y}_r(\theta), \ldots, y_r^{(l-1)}(\theta), t) \tag{9}$$

where $g_\omega(\cdot)$ is a smooth and continuous function.

In practical applications, the design of the path update law is flexible. For instance, in [5], [7], the path update law is constructed based on the error feedback.

$$\omega = -\mu_k y_r^{\theta \mathrm{T}}(\theta) s_p \tag{10}$$

where $\mu_k \in \mathbb{R}^+$ is a gain, $s_p \in \mathbb{R}^m$ is a tracking error.

In [3], the path update law is formulated to reduce the control effort via calculating the optimization problem.

$$\omega = \arg\min_{\omega} (E_g + cE_d) \tag{11}$$

where E_g is an optimization function associated with the geometric task, E_d is an optimization function associated with the dynamic task, and $c \in \mathbb{R}^+$ is a tuning weight.

In [7], [8], ω is implemented with a filter structure.

$$\begin{cases} \omega = -\rho_k h_k + \bar{\omega} \\ \dot{\bar{\omega}} = -\gamma_k(\bar{\omega} + \mu_k h_k) \\ h_k = y_r^{\theta \mathrm{T}}(\theta) s_p \end{cases} \tag{12}$$

where $\rho_k, \gamma_k, \mu_k \in \mathbb{R}^+$ are gains, $s_p \in \mathbb{R}^m$ is a tracking error. Note that these path update laws share a common characteristic: they enable the smooth updating of the path variable.

B. Parameterized path and exosystem

In this subsection, we demonstrate that the path variable can be smoothly updated using an appropriate path update law. In the geometric task of maneuvering control, the parameterized path is determined by employing various path planning methods, such as best-first searching, A*, Dijkstra, and RRT. These planning methods are capable of producing a piecewise continuous path. Consequently, in maneuvering control, the system can acquire smooth path information.

The dynamics of $y_r(\theta)$ can be extended along the dynamics of θ, but the order of $y_r(\theta)$-system should be less than the order of θ-system. Let $Y_r = [y_r^{\mathrm{T}}(\theta), \frac{dy_r^{\mathrm{T}}(\theta)}{dt}, ..., \frac{d^{k-1}y_r^{\mathrm{T}}(\theta)}{dt^{k-1}}]^{\mathrm{T}}$ and $\theta^{(k-1)} = \omega$ with $k \in \mathbb{N}^+$, the dynamics of Y_r is represented as

$$\dot{Y}_r = AY_r + B\left[f_r(\theta, y_r(\theta)) + y_r^{\theta}(\theta)\omega\right] \tag{13}$$

where

$$A = \begin{bmatrix} O_m & I_m & O_m & \cdots & O_m \\ O_m & O_m & I_m & \cdots & O_m \\ \vdots & \vdots & \ddots & \vdots & \vdots \\ O_m & O_m & O_m & \cdots & O_m \end{bmatrix} \in \mathbb{R}^{km\times km},$$

$$B = \begin{pmatrix} O_m \\ \vdots \\ O_m \\ I_m \end{pmatrix} \in \mathbb{R}^{km\times m},$$

$f_r(\theta, y_r(\theta)) \in \mathbb{R}^m$ is a known function with respect to the $(1, ..., k-2)$th order derivative of θ and the $(1, ..., k-1)$th order partial derivative of $y_r(\theta)$, and $y_r^{\theta}(\theta) \in \mathbb{R}^m$ denotes the first-order partial derivative along θ. Because the dynamics of θ is linear, a smooth ω will make the update of θ steadily, such that the parameterized path information $y_r(\theta)$ and $y_r^l(\theta)$ is also steady. When an appropriate ω is employed, the dynamics of Y_r satisfies the following form

$$\begin{cases} \dot{Y}_r(\theta) = A_Y Y_r(\theta) \\ y_r(\theta) = C_Y Y_r(\theta) \end{cases} \tag{14}$$

where

$$C_Y = \begin{bmatrix} I_m & O_m & O_m & \cdots & O_m \end{bmatrix} \in \mathbb{R}^{m\times km},$$

$$A_Y = \begin{bmatrix} O_m & I_m & O_m & \cdots & O_m \\ O_m & O_m & I_m & \cdots & O_m \\ \vdots & \vdots & \ddots & \vdots & \vdots \\ Q_{Y0} & Q_{Y1} & Q_{Y2} & \cdots & Q_{Y(k-1)} \end{bmatrix} \in \mathbb{R}^{km\times km},$$

with $Q_{Y0}, Q_{Y1}, Q_{Y2}, ..., Q_{Y(k-1)} \in \mathbb{R}^{m\times m}$ being diagonal parameter matrices. A_Y can be expressed by $A_Y = A'_Y \otimes I_m$, where the form of A'_Y satisfies

$$A'_Y = \begin{bmatrix} 0 & 1 & 0 & \cdots & 0 \\ 0 & 0 & 1 & \cdots & 0 \\ \vdots & \vdots & \ddots & \vdots & \vdots \\ -q_{Y0} & -q_{Y1} & -q_{Y2} & \cdots & -q_{Y(k-1)} \end{bmatrix} \in \mathbb{R}^{k\times k},$$

with $q_{Y0}, q_{Y1}, q_{Y2}, ..., q_{Y(k-1)} \in \mathbb{R}^+$ being tunning parameters. Eq. (14) can be regarded as an exosystem and $y_r(\theta)$ is the exogenous signal generated by this system.

C. Discussion

According to the analysis of the path variable and the desired path, it is shown that an exosystem can be established with the dynamic objective of maneuvering control. Therefore, maneuvering control can be investigated under the output regulation viewpoint. In the dynamic task, we need to construct an appropriate path update law ω to update θ smoothly, ensuring that the dynamics of the exosystem (14) remain smooth. Many existing results can achieve this task with ease. In the geometric task, we need to construct an internal model with respect to the controlled system (1). Then, the maneuvering controller can be designed to achieve the desired geometric task based on the proposed internal model and other controller design approaches.

V. An example: Neural predictor-based dynamic surface output regulation control strategy for path maneuvering problem

In this section, a neural predictor-based dynamic surface output regulation control strategy is developed for path maneuvering. To enhance the output regulation perspective, an internal model approach is used herein.

A. Neural Predictor Design

In this part, we use a full-order neural predictor to offset the adverse effects caused by the unknown dynamics. Note that many methods can also estimate or inhibit uncertain nonlinearities. At first, we can use an RBF neural network with q neurons to construct the uncertain nonlinear function $f_l(\bar{x}_l)$ as follows

$$f_l(\bar{x}_l) = W_l^{\mathrm{T}}\varphi_l(\bar{x}_l) + \varepsilon_l, \quad \bar{x}_l \subset \Omega_l \tag{15}$$

where $W_l \in \mathbb{R}^{q\times m}$ represents an output weight matrix, $\varepsilon_l \in \mathbb{R}^m$ denotes an approximation error, Ω_l denotes a compact set, and $\varphi_l(\bar{x}_l) = [\phi_1(\bar{x}_l), ..., \phi_q(\bar{x}_l)]^{\mathrm{T}} \in \mathbb{R}^q$ is the regressor vector with $\phi_l(\cdot)$ being a radial basis function. There exist positive constants W_l^*, ε_l^*, and φ_l^* such that $\|W_l\|_{\mathrm{F}} \le W_l^*$, $\|\varepsilon_l\| \le \varepsilon_l^*$, and $\|\varphi_l(\bar{x}_l)\| \le \varphi_l^*$ [16].

Based on a high gain state observer design, a full-order neural predictor is designed as follows

$$\begin{cases} \dot{\hat{x}}_k = x_{k+1} + \hat{f}_k(\bar{x}_k) - (F_k + K_k)(\hat{x}_k - x_k) \\ \dot{\hat{x}}_n = u + \hat{f}_n(\bar{x}_n) - (F_n + K_n)(\hat{x}_n - x_n) \end{cases} \tag{16}$$

where $k = 1, ..., n-1$, $\hat{f}_k(\bar{x}_k) = \hat{W}_k^{\mathrm{T}}\varphi_k(\bar{x}_k)$, $\hat{f}_n(\bar{x}_n) = \hat{W}_n^{\mathrm{T}}\varphi_n(\bar{x}_n)$, $K_k \in \mathbb{R}^{m\times m} \succ 0$ and $K_n \in \mathbb{R}^{m\times m} \succ 0$ are control gain matrices, $F_k \in \mathbb{R}^{m\times m} \succ 0$ and $F_n \in \mathbb{R}^{m\times m} \succ 0$ are tuning gain matrices. Note that the proposed method is state-feedback, where both x_l and $\hat{x}_l$ are used in the loop.

A gradient descent-based adaptation law is taken as

$$\dot{\hat{W}}_l = -\Gamma_l\left(\varphi_l(\bar{x}_l)\tilde{x}_l^{\mathrm{T}} + k_{W_l}\hat{W}_l\right), \ l = 1, ..., n \tag{17}$$

where $\tilde{x}_l = \hat{x}_l - x_l$, $\Gamma_l \in \mathbb{R}^{q\times q} \succ 0$ denotes an adaptation gain matrix, $k_{W_l} \in \mathbb{R}^{q\times q} \succ 0$ is a tuning parameter matrix.

Define $\tilde{W}_l := \hat{W}_l - W_l$. The stability of the system consisting of $\tilde{W}_l$ and $\tilde{x}_l$ can be described as follows.

Lemma 1. The system, consisting of states $\tilde{W}_l$ and $\tilde{x}_l$ and inputs W_l and ε_l, is input-to-state stable.

Proof. This lemma has been proved by some existing results in [4], [5], [7], and thus the proof is omitted to save space. $\tilde{x}_l$ can be proved satisfying $\|\tilde{x}_l\| \leq \tilde{x}_l^*$ with $\tilde{x}_l^* \in \mathbb{R}^+$ being a residual error.

B. Internal Model Design

In this part, we construct an internal model. At first, consider the following transformation along (1)

$$\begin{cases} z_1(\theta) = y_r(\theta) \\ z_2(\theta) = \dot{z}_1(\theta) - f_1(z_1) \\ z_3(\theta) = \dot{z}_2(\theta) - f_2(z_1, z_2) \\ ... \\ z_{n-1}(\theta) = \dot{z}_{n-1}(\theta) - f_{n-1}(\bar{z}_{n-1}) \\ \tau(\theta) = \dot{z}_n(\theta) - f_n(\bar{z}_n). \end{cases} \tag{18}$$

Because $f_k(\cdot)$ is an unknown nonlinear term, we construct an estimated structure for z_k using the approximation information $\hat{f}_k(\cdot)$ as follows

$$\begin{cases} \hat{z}_1(\theta) = y_r(\theta) \\ \hat{z}_2(\theta) = \dot{\hat{z}}_1(\theta) - \hat{f}_1(\hat{z}_1) \\ \hat{z}_3(\theta) = \dot{\hat{z}}_2(\theta) - \hat{f}_2(\hat{z}_1, \hat{z}_2) \\ ... \\ \hat{z}_{n-1}(\theta) = \dot{\hat{z}}_{n-1}(\theta) - \hat{f}_{n-1}(\bar{\hat{z}}_{n-1}) \\ \hat{\tau}(\theta) = \dot{\hat{z}}_n(\theta) - \hat{f}_n(\bar{\hat{z}}_n). \end{cases} \tag{19}$$

The function structures of $f_l(\bar{x}_l)$ and $f_l(\bar{z}_l)$ are same, and thus we can use the results of the full-order neural predictor $(\hat{x}_1, \hat{x}_2, ..., \hat{x}_n)$ to model $f_l(\bar{z}_l)$ as follows

$$\begin{cases} f_l(\bar{z}_l) = W_l^{\mathrm{T}} \varphi_l(\bar{z}_l) + \varepsilon_l', \quad \bar{z}_l \subset \Omega_l' \\ \hat{f}_l(\bar{z}_l) = \hat{W}_l^{\mathrm{T}} \varphi_l(\bar{z}_l). \end{cases} \tag{20}$$

Then, define $\hat{s}_k := \hat{x}_k - \hat{z}_k(\theta)$ and $s_k := x_k - \hat{z}_k(\theta)$. Wherein, the dynamics of $\hat{s}_k$ is written as follows

$$\begin{cases} \dot{\hat{s}}_k = s_{k+1} + \hat{f}_k'(\bar{\hat{z}}_k) - (F_k + K_k)\tilde{x}_k \\ \dot{\hat{s}}_n = u - \hat{\tau}(\theta) + \hat{f}_n'(\bar{\hat{z}}_n) - (F_n + K_n)\tilde{x}_n \\ y_s = s_1 \end{cases} \tag{21}$$

where $\hat{f}_l'(\bar{\hat{z}}_l) = \hat{f}_l(\bar{x}_l) - \hat{f}_l(\bar{\hat{z}}_l)$ and $\bar{\hat{z}}_l = [\hat{z}_1, ..., \hat{z}_l]^{\mathrm{T}}$ with $l = 1, ..., n$, $\hat{f}_l(\bar{\hat{z}}_l) = \hat{W}_l^{\mathrm{T}} \varphi_l(\bar{\hat{z}}_l)$. Define $\zeta(\theta) := [\hat{\tau}^{\mathrm{T}}(\theta), L\hat{\tau}^{\mathrm{T}}(\theta), ..., L^{q-1}\hat{\tau}^{\mathrm{T}}(\theta)]^{\mathrm{T}}$. The system with $\hat{\tau}(\theta)$ can be generated by the following observable linear dynamics

$$\begin{cases} \dot{\zeta}(\theta) = A_\theta \zeta(\theta) \\ \hat{\tau}(\theta) = C_\theta \zeta(\theta) \end{cases} \tag{22}$$

where

$$A_\theta = \begin{bmatrix} O_{mn} & I_{mn} & O_{mn} & \cdots & O_{mn} \\ O_{mn} & O_{mn} & I_{mn} & \cdots & O_{mn} \\ \vdots & \vdots & \ddots & \vdots & \vdots \\ A_0 & A_1 & A_2 & \cdots & A_{q-1} \end{bmatrix} \in \mathbb{R}^{mnq \times mnq},$$

$$C_\theta = \begin{bmatrix} I_{mn} & O_{mn} & O_{mn} & \cdots & O_{mn} \end{bmatrix} \in \mathbb{R}^{m \times mnq},$$

with $A_0, A_1, A_2, ..., A_{q-1} \in \mathbb{R}^{m \times m}$ being diagonal parameter matrices. There exists a state transformation for the augmented system $\eta_\theta = P_\theta \zeta(\theta)$ such that

$$\begin{cases} \dot{\eta}_\theta = (G_\theta + H_\theta \kappa_\theta)\eta_\theta \\ \hat{\tau}(\theta) = \kappa_\theta \eta_\theta \end{cases} \tag{23}$$

where the pair $(G_\theta \in \mathbb{R}^{mnq \times mnq}, H_\theta \in \mathbb{R}^{mnq \times m})$ is controllable with G_θ being Hurwitz, $\kappa_\theta = C_\theta P_\theta^{-1}$, and $P_\theta \in \mathbb{R}^{mnq \times mnq}$ is the unique solution of the following Sylvester equation

$$P_\theta A_\theta - G_\theta P_\theta = H_\theta C_\theta. \tag{24}$$

The internal model is constructed as follows

$$\dot{\xi} = (G_\theta + H_\theta \kappa_\theta)\xi + g \tag{25}$$

where g is a tuning term and to be designed later.

C. Controller Design

In this part, we use an improved DSC method to design the maneuvering controller.

Step 1. At first, we define the first error surface $\hat{e}_1 := \hat{s}_1 - s_{1d}$ with $s_{1d} := 0$. The dynamics of $\hat{e}_1$ is

$$\dot{\hat{e}}_1 = s_2 + \hat{f}_1'(\bar{\hat{z}}_1) - (F_1 + K_1)\tilde{x}_1 - \dot{s}_{1d} \tag{26}$$

To stabilize $\dot{\hat{e}}_1$, a virtual control law is constructed as

$$\alpha_2 = -K_1 e_1 - \hat{f}_1'(\bar{\hat{z}}_1) + \dot{s}_{1d} \tag{27}$$

where $e_1 = s_1 - s_{1d}$ and $K_1 \in \mathbb{R}^{m \times m} \succ 0$ is a control gain matrix. In the DSC design, the virtual control law α_2 is passed through a first-order low-pass filter or other differentiators to obtain its first-order derivative. For instance, a second-order nonlinear tracking differentiator can be used as follows [17]

$$\begin{cases} \dot{s}_{2d} = s_{2d}^{\mathrm{d}} \\ \dot{s}_{2d}^{\mathrm{d}} = -\gamma_2^2 \left\{ \beta_1 (s_{2d} - \alpha_2)^{\frac{1}{2}} + \beta_2 (\frac{v_{2d}^{\mathrm{d}}}{\gamma_2})^{\frac{2}{3}} \right\} \end{cases} \tag{28}$$

where $\gamma_2 \in \mathbb{R}^+$ denotes the time constant, $\beta_1, \beta_2 \in \mathbb{R}$ are tuning parameters. Ref. [17] proved $\|s_{2d} - \alpha_2\|$ and $\|s_{2d}^{\mathrm{d}} - \dot{\alpha}_2\|$ can converge to a small neighborhood of the origin.

Step i(i=2,3...,n-1). Define an error surface $\hat{e}_i := \hat{s}_i - s_{id}$ for the ith-order closed loop. The dynamics of $\hat{e}_i$ is

$$\dot{\hat{e}}_i = s_{i+1} + \hat{f}_i'(\bar{\hat{z}}_i) - (F_i + K_i)\tilde{x}_i - \dot{s}_{id}. \tag{29}$$

A virtual control law is constructed to stablize $\dot{e}_i$ as

$$\alpha_{i+1} = -K_i e_i - \hat{f}_i'(\bar{\hat{z}}_i) + \dot{s}_{id} - e_{i-1} \tag{30}$$

where $e_i = s_i - s_{id}$ and $K_i \in \mathbb{R}^{m \times m} \succ 0$ is a control gain matrix. Similar to *Step 1*, we can use the following second-order nonlinear tracking differentiator

$$\begin{cases} \dot{s}_{(i+1)d} = s_{(i+1)d}^{\mathrm{d}} \\ \dot{s}_{(i+1)d}^{\mathrm{d}} = -\gamma_{i+1}^2 \left\{ \beta_1 (s_{(i+1)d} - \alpha_{i+1})^{\frac{1}{2}} + \beta_2 (\frac{v_{(i+1)d}^{\mathrm{d}}}{\gamma_{i+1}})^{\frac{2}{3}} \right\} \end{cases} \tag{31}$$

where $\gamma_{i+1} \in \mathbb{R}^+$ denotes the time constant.

Step n. Define a regulation error $\Psi := \xi - \eta_\theta - H\hat{e}_n$ and the last error surface $\hat{e}_n := \hat{s}_n - s_{nd}$. The dynamics of Ψ is

$$\dot{\Psi} = (G_\theta + H_\theta\kappa_\theta)\xi + g(e_n) - (G_\theta + H_\theta\kappa_\theta)\eta_\theta - H\dot{\hat{e}}_n. \quad (32)$$

We design $g = -H_\theta K_n\hat{e}_n - (G_\theta + H_\theta\kappa_\theta)H_\theta\hat{e}_n$, and then the internal model (25) is transformed into

$$\dot{\xi} = (G_\theta + H_\theta\kappa_\theta)\xi - H_\theta K_n\hat{e}_n - (G_\theta + H_\theta\kappa_\theta)H_\theta\hat{e}_n. \quad (33)$$

The maneuvering control law is designed as follows

$$u = -K_n e_n - \hat{f}_1'(\bar{\hat{z}}_1) + \kappa_\theta\xi - \kappa_\theta H_\theta\hat{e}_n - \dot{s}_{nd} \quad (34)$$

where $e_n = s_n - s_{nd}$, $K_n \in \mathbb{R}^{m\times m} \succ 0$ is a control gain.

D. Stability Analysis

Theorem 1. Consider the uncertain nonlinear system (1). When the maneuvering controller is chosen as the internal model (25), the neural predictor (16), (17) and (20), $n-1$ virtual control laws (27) and (30), and the control law (34), the resulting closed-loop system is input-to-state stable.

Proof. Consider a Lyapunov function candidate as follows

$$V = \frac{1}{2}\sum_{k=1}^{n-1}\hat{e}_k^{\mathrm{T}}\hat{e}_k + \frac{1}{2}\Psi^{\mathrm{T}}P_\Psi\Psi \quad (35)$$

where P_Ψ is the solution of the following Lyapunov equation $G_\theta^{\mathrm{T}}P_\Psi + P_\Psi G_\theta = -2k_\theta$ with $k_\theta \in \mathbb{R}^+$ being a to-be-designed parameter. Then, $\dot{V}$ satisfies

$$\begin{aligned}\dot{V} \le &-\sum_{k=1}^{n-1}\hat{e}_k^{\mathrm{T}}K_k\hat{e}_k - \sum_{k=1}^{n-1}\hat{e}_k^{\mathrm{T}}F_k\tilde{x}_k + \sum_{k=1}^{n-1}\hat{e}_k^{\mathrm{T}}\iota_K \\ &- k_\theta\Psi^{\mathrm{T}}\Psi + \hat{e}_n^{\mathrm{T}}\kappa_\theta\Psi\end{aligned} \quad (36)$$

where $\iota_l = s_{ld} - \alpha_l$ with $l = 1, ..., n-1$. Define $\hat{E} = [\hat{e}_1^{\mathrm{T}}, \hat{e}_2^{\mathrm{T}}, ..., \hat{e}_n^{\mathrm{T}}]^{\mathrm{T}}$, $\iota = [\iota_1^{\mathrm{T}}, \iota_2^{\mathrm{T}}, ..., \iota_n^{\mathrm{T}}]^{\mathrm{T}}$, and $\tilde{X} = [\tilde{x}_1^{\mathrm{T}}, \tilde{x}_2^{\mathrm{T}}, ..., \tilde{x}_n^{\mathrm{T}}]^{\mathrm{T}}$. It follows that

$$\begin{aligned}\dot{V} \le &-\underline{\lambda}(K)\|\hat{E}\|^2 + \|\hat{E}\|\|\iota\| + \bar{\lambda}(F)\|\hat{E}\|\|\tilde{X}\| \\ &- k_\theta\Psi^{\mathrm{T}}\Psi + \Psi^{\mathrm{T}}HF_n\tilde{x}_n + \hat{e}_n^{\mathrm{T}}\kappa_\theta\Psi\end{aligned} \quad (37)$$

where $\iota_l = s_{ld} - \alpha_l$ with $l = 1, ..., n-1$, $K = \mathrm{diag}\{K_1, ..., K_n\}$, $F = \mathrm{diag}\{F_1, ..., F_n\}$. Using the following Young's inequality

$$\hat{e}_n^T\kappa_\theta\Psi \le \frac{1}{2}\|\hat{e}_n\|^2 + \frac{\bar{\lambda}(\kappa_\theta)}{2}\|\Psi\|^2 \le \frac{1}{2}\|\hat{E}\|^2 + \frac{\bar{\lambda}(\kappa_\theta)}{2}\|\Psi\|^2$$

It follows that

$$\begin{aligned}\dot{V} \le &-(\underline{\lambda}(K) - \frac{1}{2})\|\hat{E}\|^2 - (k_\theta - \frac{\bar{\lambda}(\kappa_\theta)}{2})\|\Psi\|^2 \\ &+ \|\hat{E}\|\|\iota\| + \bar{\lambda}(F)\bar{\lambda}(H_\theta)\|\Psi\|\|\tilde{X}\| \\ \le &-c_\theta\|X_\theta\|^2 + d_\theta\|X_\theta\|\|U_\theta\|\end{aligned} \quad (38)$$

where $X_\theta = [\|\hat{E}\|, \|\Psi\|]^{\mathrm{T}}$, $U_\theta = [\|\iota\|, \|\tilde{X}\|]^{\mathrm{T}}$, $c_\theta = \min\{\underline{\lambda}(K) - 0.5, k_\theta - 0.5\bar{\lambda}(\kappa_\theta)\}$, $d_\theta = 1 + \bar{\lambda}(F) + \bar{\lambda}(F)\bar{\lambda}(H_\theta)$.

Since $\|X_\theta\| \ge 2d_\theta\|X_\theta\|/c_\theta$ makes $\dot{V} \le -0.5c_\theta\|X_\theta\|^2$, the closed loop system is input-to-state stable. For all $t > t_0$, there exist a class $\mathcal{KL}$ function $\beta(\cdot)$ and two class $\mathcal{K}_\infty$ functions $g_\iota(\cdot)$ and $g_{\tilde{X}}(\cdot)$, and $\|X_\theta\|$ satisfies

$$\|X_\theta(t)\| \le \beta(\|X_\theta(t_0)\|, t - t_0) + g_\iota(\|\iota\|) + g_{\tilde{X}}(\|\tilde{X}\|). \quad (39)$$

Lemma 1 has shown that the system $(\tilde{x}_l, \tilde{W}_l)$ is input-to-state stable. Based on the cascade system analysis, Eq. (39) can be further put into

$$\begin{aligned}\|X_\theta(t)\| &\le \beta(\|X_\theta(t_0)\|, t - t_0) + g_\iota(\|\iota\|) + \sum_{i=1}^{M} g_{\tilde{X}}(\|\tilde{x}_i\|) \\ &\le \beta(\|X_\theta(t_0)\|, t - t_0) + g_\iota(\|\iota\|) \\ &\quad + \sum_{i=1}^{M} g_{\tilde{x}_i} \circ (g_{W_i}(\|W_i\|_{\mathrm{F}}) + g_{\varepsilon_i}(\|\varepsilon_i\|)\end{aligned} \quad (40)$$

where $g_{W_i}(\cdot)$ and $g_{\varepsilon_i}(\cdot)$ are two class $\mathcal{K}_\infty$ functions.

Remark 1. Theorem 1 gives a brief proof to demonstrate the input-to-state stability of the closed-loop system in relation to the geometric task. It is shown by this theorem that the output regulation-based maneuvering controller has similar stability results to those of existing results in [4]–[9].

VI. Simulation results

In this part, we will use the proposed strategy to design a controller to achieve the parameterized path-guided maneuvering control. Consider the following uncertain system

$$\begin{cases} \dot{x}_{1,1} = x_{2,1} + 2x_{1,1}^2 + x_{1,2} \\ \dot{x}_{1,2} = x_{2,2} + \cos(x_{1,1} + x_{1,2}) \\ \dot{x}_{2,1} = u_1 + \sin(x_{1,1}^2 + x_{2,1}) + \cos(x_{2,2}^2) \\ \dot{x}_{2,2} = u_2 + \cos(2x_{1,2} + x_{2,1} + x_{2,2}) \\ y = x_1 \end{cases} \quad (41)$$

where $[x_{1,1}, x_{1,2}]^{\mathrm{T}} = x_1$ and $[x_{2,1}, x_{2,2}]^{\mathrm{T}} = x_2$ are states, $[u_1, u_2]^{\mathrm{T}} = u$ is the control input, and y denotes the output. The uncertain nonlinear system is driven to track the parameterized path $y_r(\theta) = [\sin(\theta), \cos(\theta)]^{\mathrm{T}}$ with $v_s = 0.45$. In this simulation, we use the path update law (42) in [4] for convenience. The simulation parameters are chosen as $K_1 = \mathrm{diag}\{6, 6\}$, $K_2 = \mathrm{diag}\{15, 15\}$, $\gamma_1 = 20$, $\Gamma_1 = \Gamma_2 = \mathrm{diag}\{5000, 5000\}$, $K_{W_1} = K_{W_2} = \mathrm{diag}\{5\times10^{-6}, 5\times10^{-6}\}$, $F_1 = \mathrm{diag}\{204, 204\}$, and $F_2 = \mathrm{diag}\{485, 485\}$.

Define $\zeta(\theta) = [\hat{\tau}^{\mathrm{T}}(\theta), L\hat{\tau}^{\mathrm{T}}(\theta)]^{\mathrm{T}} \in \mathbb{R}^4$. The system with $\hat{\tau}(\theta)$ can be generated by the following linear system

$$\begin{cases} \dot{\eta}(\theta) = A_\theta\eta(\theta) \\ \hat{\tau}(\theta) = C_\theta\eta(\theta) \end{cases} \quad (42)$$

where

$$A_\theta = \begin{bmatrix} 0 & 0 & 1 & 0 \\ 0 & 0 & 0 & 1 \\ -17 & 0 & -32 & 0 \\ 0 & -17 & 0 & -32 \end{bmatrix}.$$

Let

$$G_\theta = \begin{bmatrix} 0 & 0 & 1 & 0 \\ 0 & 0 & 0 & 1 \\ -15 & 0 & -15 & 0 \\ 0 & -15 & 0 & -15 \end{bmatrix}, H_\theta = \begin{bmatrix} 0 & 0 \\ 0 & 0 \\ 1 & 0 \\ 0 & 1 \end{bmatrix},$$

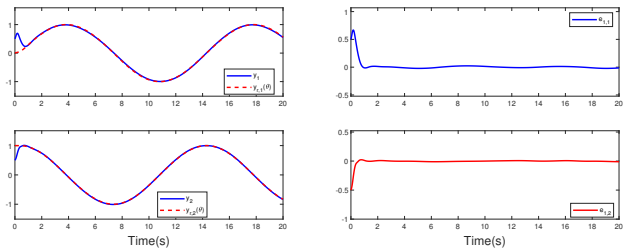

(a) (b)

Fig. 1: Maneuvering control performance: (a) Output of the controlled system y; (b) Maneuvering error in two dimensions e_1.

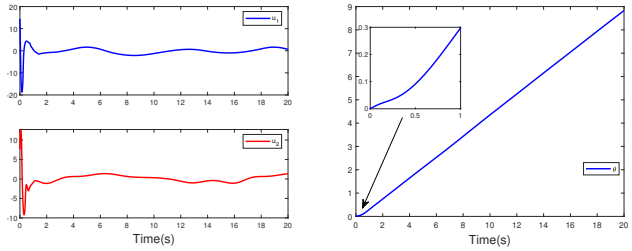

(a) (b)

Fig. 2: Control efforts: (a) Control input of the system u; (b) Evolution of the path variable θ.

P_θ can be calculated as

$$P_\theta = \begin{bmatrix} 0.1416 & 0 & 0.0044 & 0 \\ 0 & 0.1416 & 0 & 0.0044 \\ -0.0755 & 0 & -0.0005 & 0 \\ 0 & -0.0755 & 0 & -0.0005 \end{bmatrix}.$$

The internal model is designed as

$$\dot{\xi} = \begin{bmatrix} 0 & 0 & 1 & 0 \\ 0 & 0 & 0 & 1 \\ -17 & 0 & -32 & 0 \\ 0 & -17 & 0 & -32 \end{bmatrix} \xi + \begin{bmatrix} 1 & 0 \\ 0 & 1 \\ 10 & 0 \\ 0 & 10 \end{bmatrix} \hat{e}_2. \quad (43)$$

The initial values of state variables in the controller are: $x_1(0) = \hat{x}_1(0) = s_{2d}(0) = [0.5, 0.5]^{\mathrm{T}}$, $x_2(0) = \hat{x}_2(0) = s_{2d}^d(0) = [0, 0]^{\mathrm{T}}$, $\xi(0) = [0, 0, 0, 0]^{\mathrm{T}}$.

It is shown in Fig. 1(a) that the output y can track the given parameterized path using the proposed controller. In Fig. 1(b), we can observe that the maneuvering error can converge to a residual error near the origin. Therefore, the geometric task of maneuvering control can be achieved. Fig. 2(a) depicts the evolution of the control input u. Fig. 2(b) shows the smooth update of the path variable θ, satisfying the dynamic task of the maneuvering control.

VII. Conclusion

In this paper, we attempted to investigate the maneuvering control problem of a class of uncertain nonlinear systems from the perspective of output regulation. We demonstrated that a path update law satisfying dynamic objectives of maneuvering control can transform the dynamics of the desired path into those of a smooth and continuous exosystem, where the parameterized path can serve as an exogenous signal. Based on this issue, we designed a neural predictor-based DSC output regulation control strategy as an example. The closed-loop system in relation to the geometric task was proven to be input-to-state stable, and a numerical simulation example was provided to show the effectiveness of the proposed theoretical results. In the future, we will further refine this perspective and apply it to solve cooperative maneuvering control problems.

References

[1] J. Hauser and R. Hindman, "Maneuver regulation from trajectory tracking: Feedback linearizable systems," *Proceedings of the IFAC symposium on nonlinear control systems design*, pp. 595–600, 1995.

[2] R. Skjetne, T. I. Fossen, and P. V. Kokotović, "Robust output maneuvering for a class of nonlinear systems," *Automatica*, vol. 40, no. 3, pp. 373–383, Mar 2004.

[3] D. B. Dacic, M. V. Subbotin, and P. V. Kokotovic, "Control effort reduction in tracking feedback laws," *IEEE Transactions on Automatic Control*, vol. 51, no. 11, pp. 1831–1837, Nov 2006.

[4] Y. Zhang, D. Wang, and Z. Peng, "Consensus maneuvering for a class of nonlinear multivehicle systems in strict-feedback form," *IEEE Transactions on Cybernetics*, vol. 49, no. 5, pp. 1759–1767, 2019.

[5] Y. Zhang, D. Wang, Z. Peng, and T. Li, "Distributed containment maneuvering of uncertain multiagent systems in mimo strict-feedback form," *IEEE Transactions on Systems, Man, and Cybernetics: Systems*, vol. 51, no. 2, pp. 1354–1364, 2021.

[6] Y. Zhang, W. Wu, W. Chen, H. Lu, and W. Zhang, "Output-feedback consensus maneuvering of uncertain mimo strict-feedback multiagent systems based on a high-order neural observer," *IEEE Transactions on Cybernetics*, vol. 54, no. 7, pp. 4111–4123, 2024.

[7] Z. Peng, J. Wang, and D. Wang, "Containment maneuvering of marine surface vehicles with multiple parameterized paths via spatial-temporal decoupling," *IEEE/ASME Transactions on Mechatronics*, vol. 22, no. 2, pp. 1026–1036, Apr 2017.

[8] ——, "Distributed containment maneuvering of multiple marine vessels via neurodynamics-based output feedback," *IEEE Transactions on Industrial Electronics*, vol. 65, no. 4, pp. 3831–3839, May 2017.

[9] N. Gu, D. Wang, Z. Peng, and J. Wang, "Safety-critical containment maneuvering of underactuated autonomous surface vehicles based on neurodynamic optimization with control barrier functions," *IEEE Transactions on Neural Networks and Learning Systems*, vol. 34, no. 6, pp. 2882–2895, 2023.

[10] T. Faulwasser, T. Weber, P. Zometa, and R. Findeisen, "Implementation of nonlinear model predictive path-following control for an industrial robot," *IEEE Transactions on Control Systems Technology*, vol. 25, no. 4, pp. 1505–1511, 2017.

[11] S. Wu, X. Liang, Y. Fang, and W. He, "Geometric maneuvering for underactuated vtol vehicles," *IEEE Transactions on Automatic Control*, vol. 69, no. 3, pp. 1507–1519, 2024.

[12] P. Sujit, S. Saripalli, and J. B. Sousa, "Unmanned aerial vehicle path following: A survey and analysis of algorithms for fixed-wing unmanned aerial vehicless," *IEEE Control Systems Magazine*, vol. 34, no. 1, pp. 42–59, 2014.

[13] J. Huang and Z. Chen, "A general framework for tackling the output regulation problem," *IEEE Transactions on Automatic Control*, vol. 49, no. 12, pp. 2203–2218, 2004.

[14] Y. Dong, J. Chen, and J. Huang, "Cooperative robust output regulation for second-order nonlinear multiagent systems with an unknown exosystem," *IEEE Transactions on Automatic Control*, vol. 63, no. 10, pp. 3418–3425, Oct. 2018.

[15] Y. Hao, J. Zhang, and L. Liu, "Fully distributed event-triggered cooperative output regulation of multiagent systems under jointly connected digraphs," *IEEE Transactions on Automatic Control*, vol. 68, no. 7, pp. 4241–4248, 2023.

[16] A. Kurdila, F. J. Narcowich, and J. D. Ward, "Persistency of excitation in identification using radial basis function approximants," *SIAM journal on control and optimization*, vol. 33, no. 2, pp. 625–642, 1995.

[17] B. Guo and Z. Zhao, "Weak convergence of nonlinear high-gain tracking differentiator," *IEEE Transactions on Automatic Control*, vol. 58, no. 4, pp. 1074–1080, Apr 2013.